Estimation of Spatial Degrees of Freedom of a Climate Field

XIAOCHUN WANG

Department of Meteorology, School of Ocean and Earth Science and Technology, University of Hawaii at Manoa, Honolulu, Hawaii

SAMUEL S. SHEN

Department of Mathematical Sciences, University of Alberta, Edmonton, Alberta, Canada

(Manuscript received 19 September 1997, in final form 1 June 1998)

ABSTRACT

This paper analyzes four methods for estimating the spatial degrees of freedom (dof) of a climate field: the χ^2 method, the Z method, the S method, and the B method. The results show that the B method provides the most accurate estimate of the dof. The χ^2 method, S method, and Z method yield underestimates when the number of realizations of the field is not sufficiently large or the field's mean and variance vary with respect to spatial location. The dof of the monthly surface temperature field is studied numerically. The B method shows that the dof of the Northern Hemisphere (NH) has an obvious annual cycle, which is around 60 in the winter months and 90 in the summer months. The dof for the Southern Hemisphere (SH) varies between 35 and 50, with large values during its winter months and small ones during its summer months. The dof of the global temperature field demonstrates a similar annual cycle to that of the NH. The dof estimated from the observational data is smaller than that from the GFDL GCM model output of the surface air temperature. In addition, the model output for the SH shows the opposite phase of the seasonal cycle of the dof: large dof in summer and small ones in winter.

1. Introduction

Because of spatial correlations among different locations (and also temporal autocorrelation at one location), the value of ''spatial degrees of freedom'' or ''effective number of independent sites'' is often less than the number of the spatial grid points in a climate field. If a specific statistic (e.g., variance) of the field is estimated by using a group of independent random variables and the two statistics are made equal, the number of the independent variables is defined as the spatial degrees of freedom (dof) of the field (Thiébaux and Zwiers 1984). Therefore, the dof depends on the sample statistic used for its estimation. Many recent papers investigated the methods of dof estimation and their applications (e.g., Jones et al. 1997; Toth 1995; Fraedrich et al. 1995). The present paper analyzes four methods and uses the most accurate and robust one to calculate the dof of both the observed and GCM-generated monthly surface temperature.

The importance of the dof is twofold. First, the dof is an index of a climate field's complexity. The dof is mainly related to the covariance matrix of the climate field, which can be represented by the superposition of its EOFs and the corresponding variances (Shen et al. 1994). The dof is, therefore, a useful index to measure the discrepancy between the GCM output and the observational data (Fraedrich et al. 1995; Van den Dool and Chervin 1986). Another example is the question of how many stations are needed to measure the global average annual mean surface temperature. Researchers previously believed that an accurate estimate required a large number of observations. Jones et al. (1986a,b), Hansen and Lebedeff (1987), and Vinnikov et al. (1990) used more than 500 stations. However, researchers gradually realized that the global surface temperature field has a very low dof. For observed seasonal average temperature, the dof are around 40 (Jones et al. 1997), and one estimate for GCM output is 135 (Madden et al. 1993). Jones (1994) showed that the average temperature of the Northern (Southern) Hemisphere estimated with 109 (63) stations was satisfactorily accurate when compared to the results from more than 2000 stations. Shen et al. (1994) showed that the global average annual mean surface temperature can be accurately estimated by using around 60 stations, well distributed on the globe, with an optimal weight for each station. Second, to perform some statistical testings, an a priori knowledge of the dof of the field is needed, such as finding

Corresponding author address: Mr. Xiaochun Wang, Department of Meteorology, University of Hawaii at Manoa, 2525 Correa Road, Honolulu, HI 96822.
E-mail: xiao@kukui.soest.hawaii.edu

© 1999 American Meteorological Society

the significance of CO_2-related or solar-related climate changes (Livezey and Chen 1983). Another example was given by Bell (1986), showing that for the finite number of realizations of a climate field, the chances of detecting a climate signal is reduced when too many correlated variables or too few independent variables are included in the detection scheme [see Fig. 5 of Bell (1986)].

At least a half-a-dozen different methods were proposed to estimate a field's dof. Four of them are simple in theory and stable in computation and, hence, have been chosen for analysis in this paper. The first one is based on the idea that the difference between two realizations of a field satisfies a normal distribution; hence, the averaged sum of the squared differences should satisfy the chi-square distribution. Comparing the data distribution of the mean square difference with the distribution function of a chi-square variable with a known dof, the closest fit between the data and the distribution function determines the dof of the field in question (Lorenz 1969; Toth 1995). Fraedrich et al. (1995) considered the second moment fit and derived an analytic formula of the dof estimation. The second method is based on the binomial distribution (Livezey and Chen 1983). The third one uses the Fisher Z transformation (Horel 1985; Van den Dool and Chervin 1986). The variance of the correlation coefficient between two realizations of a field after the Fisher Z transformation should be $1/(n - 3)$, where n is the number of independent variables in the field (Sachs 1984). The fourth method is based on the idea of random sampling; that is, the sample mean has less variance than the individual samples do (Smith et al. 1994).

In addition to the above four methods, other methods exist, such as the correlation decay length method (Jones et al. 1997; Madden et al. 1993) and the hyperspheres method (Toth 1995). In the former method, a homogeneous and isotropic correlation function model is used for the field, and the results of the dof estimation depend upon the correlation function model. However, the true correlation is neither homogeneous nor isotropic and varies with spatial locations (see, e.g., Kim and North 1991). The hyperspheres method of Toth (1995) fits a distribution function by data and is an alteration of the chi-square method.

This paper will investigate only the first four methods and refer to them as the χ^2 method (chi-square method), the Z method (Z transformation method), the S method (random sampling method), and the B method (binomial distribution method). Rather than discussing the mathematical theory of dof estimation, this paper focuses on the application of these methods. Our objectives are to compare different methods of dof estimation, to propose a plausible method for the dof estimation of a climate field, and to apply this method to the observational data and GCM output. The four methods are compared by using randomly generated data and surface temperature observations. Based on the comparison, a modified B method for dof estimation is proposed. The proposed method is applied to both the observational and GCM output of surface temperature. Comparisons of the dof estimation, between the Northern Hemisphere and the Southern Hemisphere and between the observational data and GCM output, provide further insight into the surface temperature field and the performance of the GCM.

The outline of the paper is as follows. The theories of the four dof estimation methods are briefly presented in section 2. Section 3, using randomly generated data, describes the pros and cons of these four methods. The nature of data used in the analysis is explained in section 4. Section 5 presents the dof estimation from observational surface temperature. The dof estimation from GCM output is given in section 6. The conclusions and discussions are in section 7.

2. Methods for dof estimation

In this section, we review the four methods for dof estimation investigated in this paper. We use different notations to represent a climate field in order to facilitate our discussion. A climate field can be treated either as the realizations of a group of N dependent random variables or as the realizations of a random vector $\mathbf{x}$ with dimension N. In application, a climate field is represented as a two-dimensional matrix $[\mathbf{X}]$ with elements $x_{i,t}$; $i = 1, \ldots, N$, $t = 1, \ldots, T$; where N is the number of spatial points and T is the number of realizations or the temporal length of the field.

a. The chi-square method

The χ^2 method (chi-square method) uses the distribution of the squared difference between realizations of a field or between a realization and the climatology. If the difference field is normally distributed at each spatial location, the sum of the squared differences of the field at all spatial locations is a chi-square variable. Lorenz (1969) and Toth (1995) fitted the sum of the squared differences to the chi-square distribution function, which is determined by its dof. The best fit gave the dof of the field. Fraedrich et al. (1995) used the second moment fitting and derived an analytic formula for the dof.

Let X_i ($i = 1, \ldots, N$) be normally distributed variables satisfying $\mathcal{N}(0, 1)$. The second moment fitting implies that

$$\mathrm{var}\left(\frac{\sum_{i=1}^{N} X_i^2}{N}\right) = \mathrm{var}\left(\frac{\chi^2_{\mathrm{dof}}}{\mathrm{dof}}\right), \tag{1}$$

where χ^2_{dof} is a chi-square variable with its degrees of freedom as dof. The right-hand side of the above is

$$\mathrm{var}\left(\frac{\chi^2_{\mathrm{dof}}}{\mathrm{dof}}\right) = \frac{\mathrm{var}(\chi^2_{\mathrm{dof}})}{\mathrm{dof}^2} = \frac{2}{\mathrm{dof}}.$$

Using the empirical orthogonal function representation of the covariance matrix of these variables, one can have

$$\mathrm{var}\left(\sum_{i=1}^{N} X_i^2\right) = 2\sum_{k=1}^{N} \lambda_k^2.$$

The above three expressions lead to the following analytic dof-estimation formula:

$$\mathrm{dof} = N^2 \Big/ \sum_{k=1}^{N} \lambda_k^2, \tag{2}$$

where λ_k ($k = 1, \ldots, N$) are the eigenvalues of the covariance matrix. When the number of realizations of a field is not sufficiently large, the replacement of the ensemble average by the arithmetic average of the finite realizations may result in errors in the eigenvalue calculation. The error may be regarded as a perturbation of the eigenvalue due to insufficient ensemble samplings. North et al. (1982) derived a formula for the perturbation,

$$\Delta\lambda_k \approx \lambda_k(2/M)^{1/2},$$

where M is the number of independent realizations of the climate field. The differential of the formula (2) should yield the perturbation of the dof:

$$\Delta\mathrm{dof} = -\frac{N^2}{\left(\sum_{k=1}^{N} \lambda_k^2\right)^2} \sum_{k=1}^{N} 2\lambda_k\Delta\lambda_k = -2\left(\frac{2}{M}\right)^{1/2}\mathrm{dof}.$$

In this way, an estimation of the lower and upper bounds of the dof is obtained:

$$\mathrm{dof}_{\pm} = \mathrm{dof} \pm \Delta\mathrm{dof} = [1 \mp 2(2/M)^{1/2}]\mathrm{dof}. \tag{3}$$

This formula differs slightly from that of Fraedrich et al. (1995). Since the result of North et al. (1982) is a perturbation result, the bounds given by (3) can be regarded only as a reference instead of a confidence interval. Generally M is less than the temporal length T and can be estimated by using the method for estimating the effective sample size of a time series (Thièbaux and Zwiers 1984). A small M produces a large sampling error in the estimation of eigenvalues, hence a large uncertainty in the estimation of the dof. For example, when M is 40, the lower and upper bounds of the dof are

$$(\mathrm{dof}_-, \mathrm{dof}_+) = (0.55, 1.45)\mathrm{dof}. \tag{4}$$

b. The Z method

The pattern correlation coefficients between two realizations of a field after the Fisher Z transformation are from a normally distributed population whose variance depends on the dof of the field (Sachs 1984, 427). Namely, the variable

$$\xi = \frac{1}{2}\log\left(\frac{1 + r}{1 - r}\right) \tag{5}$$

is normally distributed, where r is the pattern correlation coefficient between two realizations of the field. The variance of variable ξ is

$$\mathrm{var}(\xi) = (\mathrm{dof} - 3)^{-1}; \tag{6}$$

hence the dof can be estimated if the variance of the Fisher Z transformed pattern correlation coefficient is known. However, computations of the pattern correlation coefficient r between two realizations of the field assume that the climate field at different spatial locations satisfies the same distribution. This homogeneity assumption is often problematic for a true climate field, since it has a different variance and mean at different spatial locations. In our analysis, the standardized climate field (standardized by its mean and standard deviation at each location) is used, such that the transformed data are closer to being homogeneous.

c. The S method

For a group of independent random variables of size n (Y_i, $i = 1, \ldots, n$) with mean μ and variance σ^2, the sample mean $(1/n)\ \Sigma_{i=1}^{n} Y_i$ has a variance

$$\mathrm{var}\left(\frac{1}{n}\sum_{i=1}^{n} Y_i\right) = \frac{1}{n}\sigma^2.$$

In this case, n is the dof of these random variables (since they are independent). For a climate field X_i ($i = 1, \ldots, N$) of normal distribution with $\mathrm{var}(X_i) = \sigma_i^2$ and $\langle X_i\rangle = \mu_i$, the variance of the field's average is less than the average of the variance field. The S method assumed that the ratio of the two should be the dof:

$$\sigma_T^2 = \overline{\sigma}^2/\mathrm{dof}, \tag{7}$$

where

$$\sigma_T^2 = \mathrm{var}(\overline{X}) = \mathrm{var}\left(\frac{\sum_{i=1}^{N} X_i}{N}\right), \tag{8}$$

$$\overline{\sigma}^2 = \frac{\sum_{i=1}^{N} \mathrm{var}(X_i)}{N}. \tag{9}$$

Another way to estimate σ_T^2 is as follows:

$$\sigma_T^2 = E[(\overline{X} - \overline{\mu})^2], \tag{10}$$

where $\overline{\mu}$ is the mean of the expected values of all spatial locations. By using $\overline{X} = (1/N)\ \Sigma_{i=1}^{N} X_i$ and $\overline{\mu} = (1/N)\ \Sigma_{i=1}^{N} E[X_i]$, the expansion of (10) yields

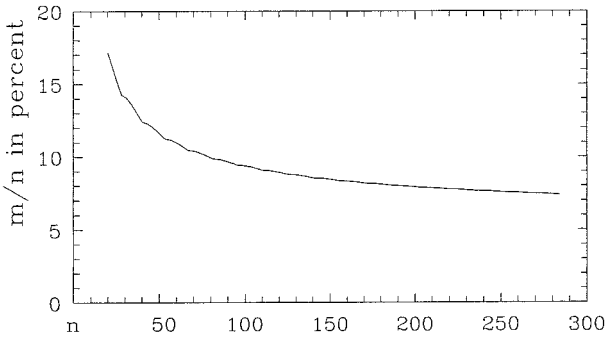

FIG. 1. The m/n in percentage as a function of n for the binomial distribution $B(n, p)$, when $p = 0.05$, $P_B = 0.05$ such that $P(X \geq m) = P_B$. The abscissa denotes n and the ordinate is m/n in percent.

$$\sigma_T^2 = \frac{1}{N^2} E\left[\sum_{i=1}^{N} (X_i - \mu_i)\right]^2 = \frac{1}{N^2}\left[\sum_{i=1}^{N} \sigma_i^2 + 2\sum_{i=1}^{N-1}\sum_{j=i+1}^{N} \mathrm{cov}(X_i, X_j)\right], \quad (11)$$

where $\mathrm{cov}(X_i, X_j)$ is the covariance between X_i and X_j. Equating (7) and (10) provides a dof estimate,

$$\mathrm{dof} = N\left(\sum_{i=1}^{N} \sigma_i^2\right)\left[\sum_{i=1}^{N} \sigma_i^2 + 2\sum_{i=1}^{N-1}\sum_{j=i+1}^{N} \mathrm{cov}(X_i, X_j)\right]^{-1}. \quad (12)$$

Smith et al. (1994) used the method on a global sea surface temperature field. The estimated dof's varied from 5 to 53 for different datasets from a 10-yr period. If the region concerned is not very large, in which case the mean and variance of the field do not vary significantly, the method may be plausible. If the region concerned is hemispheric or global, the method will introduce a large error, so that once again, inhomogeneity causes problems.

d. The B method

The B method estimates the dof of a climate field [**X**] by using the binomial distribution (Livezey and Chen 1983). The sample statistic used in the B method is the ratio of the number of successful Bernoulli trials (m_0, defined later) to the number of spatial points (N). For a binomial distribution, $B(n, p)$, an m can be decided for a given probability, P_B, such that $P(X \geq m) = P_B$. For example, if the number of trials is $n = 30$, the probability of success for each trial is $p = 0.05$, and the given probability is $P_B = 0.05$; then $\int_{4.24}^{\infty} B(30, 0.05)(x)\, dx = 0.05$ leads to $m = 4.24$ and $m/n = 14.13\%$. The number of independent trials n in the B method is regarded as the number of independent spatial locations, that is, the dof. Hence, the above relationship between m/n and n (see Fig. 1) can be used to estimate the dof of the field. The B method's procedure has two steps: (i) using the Monte Carlo method to determine m_0/N and (ii) using the relation between m/n and n to determine n.

The B method uses the significance tests of correlation coefficients as Bernoulli trials. Suppose that a time series R_t ($t = 1, \ldots, T$) is randomly generated according to normal distribution $\mathcal{N}(0, 1)$, and the correlation coefficient between R_t and the climatic data at a given point (i.e., those elements $x_{i,t}$ of [**X**] when i is a spatial index and $t = 1, \ldots, T$) is calculated. Then the pass or failure of the correlation coefficient test for significance level p is a Bernoulli trial. Using the Monte Carlo simulation, a large number of simulations, say S, provide an estimate of m/n by m_0/N, where m_0 is estimated from the distribution of Monte Carlo simulations by

$$P(X \geq m_0) = P_B. \quad (13)$$

Upon obtaining m_0/N, by equating m_0/N to m/n, the number of independent grid points can be estimated from the relationship of m/n and n (i.e., dof $= n$).

In principle, the selection of P_B and p does not affect the estimation of the dof. But intuitively, P_B and (especially) S should be large so that $P_B \times S$ is sufficiently large. In the following computation, we select P_B as 0.05 and p as 0.05. Figure 1 presents m/n in percentage as a function of n when $P_B = 0.05$ and $p = 0.05$, demonstrating that a small n (e.g., less than 100) provides relatively large differences in m/n for different n. When n changes from 40 to 60, m/n changes from 12.45% to 10.98%. When n is large, say, greater than 150, the variation of m/n is very small. For example, when n changes from 160 to 180, m/n changes from 8.32% to 8.10%. Thus, for a larger n, the B method will rely on the estimation of m_0. Since the B method is based on the estimation of m/n in order to provide an estimate of the dof, the number of Monte Carlo simulations should be sufficiently large so that a robust estimate can be achieved. In the next section, further analysis of the influence of the number of Monte Carlo simulations on the dof estimation will be made, and a feasible computational procedure will be proposed.

3. Comparison of dof estimation methods

Numerical experiments are conducted to compare the accuracy and robustness of dof estimation methods. With the exception of section 3d, for most experiments we start with a 100×40 data matrix randomly generated according to standard normal distribution $\mathcal{N}(0, 1)$, with 100 as the number of spatial points and 40 as the number of realizations of the field. By definition, the dof of the data matrix is 100.

a. The χ^2 method

Section 2a pointed out that the sampling errors of the eigenvalues of the covariance matrix may affect dof estimation. A group of numerical experiments were car-

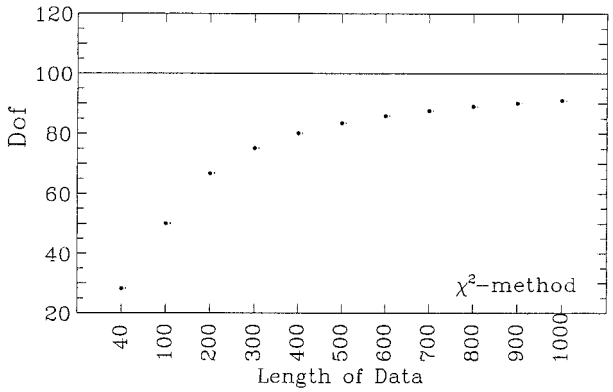

FIG. 2. The means (dots) and standard deviations (short vertical lines beside the dots) of dof estimates using the χ^2 method for randomly generated standard normal distribution data. The abscissa is the length of data or the number of realizations, and the ordinate denotes dof. The real dof of the data (100) is shown as a straight line. For details, see section 3a.

ried out to analyze the effect. In the experiments, the number of realizations of the field was gradually increased from 40 to 1000. For each fixed number of realizations, 100 experiments were conducted by randomly generating a field and estimating its dof by the χ^2 method. Then the mean and standard deviation of the dof estimates were computed. The mean and standard deviation of the dof estimates are shown in Fig. 2 as functions of the number of realizations, that is, the length of data. Figure 2 indicates that when the length of data is short, a large sampling error results in the eigenvalue estimate of covariance matrix, hence, a large error in dof estimation. When the length of data is 40, the estimated dof is 28. The ratio of the estimated dof and true dof (100) is 0.28. The true dof is not even in the interval of formula (4). As the length of data increases, the estimated dof gradually approaches the true dof. The estimated dof is 91 and very close to the true dof when the length of data is 1000. In all the experiments, the estimated dof's are always less than the true dof. The standard deviation of dof's estimated by the χ^2 method are generally less than 0.5 when the length of data changes from 40 to 1000, possibly because the χ^2 method uses an explicit formula for the dof. So for dof estimation of a climate field, the χ^2 method needs a large number of realizations or a long time series. Unfortunately, the requirement cannot be met by observational data that have a typical length of several decades.

b. The Z and S methods

For the Z method, we still start with a 100×40 data matrix, as described in the beginning of section 3. The variance of variable ξ is estimated by using the Fisher Z transformed correlation coefficients, which have a total number of 780 [i.e., $\binom{40}{2}$] for the data matrix. The dof is estimated by formula (6). The above procedure is repeated 100 times. Each time, a new data matrix is randomly generated, and its dof is estimated by the Z method. The mean and standard deviation of the estimated dof's are 102 and 5, respectively. At first, the Z method appears to be a reasonable way to estimate the dof, but when the data for each spatial location does not satisfy $\mathcal{N}(0, 1)$, the estimated dof has a significant deviation from the true dof.

A data matrix [**F**] is generated as

$$f_{i,t} = a_i X_t + 0.1a_i, \tag{14}$$

in which $i = 1, \ldots, 100$; $t = 1, \ldots, 40$; a_i is a constant; and X_t is an $\mathcal{N}(0, 1)$ random variable. The dof estimation is conducted 100 times. Each time, a data matrix [**F**] is generated, and its dof is estimated by the Z method. Since X_t is an $\mathcal{N}(0, 1)$ random variable, [**F**] obviously still has a dof of 100. But for different i, $f_{i,t}$ is a random variable with its mean and variance as $0.1a_i$ and a_i^2, respectively. The results show that the estimated dof using the Z method for 100 experiments has a mean of 57 and a standard deviation of 5. The ratio of the estimated dof to the true value (100) is 0.57. If the χ^2 method is used in this experiment, the estimated dof is 28. The experiment shows that if the mean and variance change with spatial location, the estimated dof using the Z method will have a significant error. An interesting point is that both the Z method and χ^2 method cause an underestimation.

For the S method, the experiment with a 100×40 data matrix is also conducted. The mean and standard deviation of dof estimates for data satisfying standard normal distribution are 108 and 26, respectively. However, if the data generated according to formula (14) are used, the mean and standard deviation of dof estimates are 82 and 11. For a climate field in which mean and variance change with spatial location, the S method also yields a dof estimate with a large error.

c. The B method

As section 2 points out, dof estimation using the B method may be influenced by the estimation of m/n, especially when the number of Monte Carlo simulations is not large enough. In the following experiment, the number of Monte Carlo simulations is increased gradually from 100 to 3000. For each fixed number of Monte Carlo simulations, the estimation is repeated 100 times for the same field. The mean and standard deviation of the estimated dof's are shown in Fig. 3 as functions of the number of Monte Carlo simulations. For a 100×40 dataset when the number of Monte Carlo simulations is 100, the mean and standard deviation of the estimated dof are, respectively, 106 and 24. When the number of Monte Carlo simulations increases, the estimated dof moves even closer to the true dof. The mean and standard deviation of the estimated dof's are 99 and 5 when the number of Monte Carlo simulations is 3000.

Another interesting feature of Fig. 3 is that while the

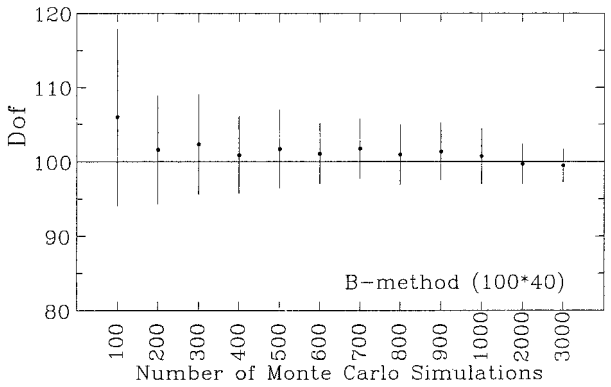

FIG. 3. The means (dots) and standard deviations (vertical lines) of dof estimates obtained by the B method for a randomly generated standard normal distribution data matrix (100 × 40) with a different number of Monte Carlo simulations. The abscissa denotes the number of Monte Carlo simulations, and the ordinate is the dof. The real dof is shown as a straight line.

χ^2 method, Z method, and S method yield very low underestimates of the dof, when the length of data is not sufficiently long or the mean and variance of the field change with spatial location, the B method can provide more accurate dof estimates. It should also be noted that for the data matrix generated according to formula (14), the mean and standard deviation of the estimated dof's provided by the B method are 101 and 7, with the number of Monte Carlo simulations as 1000 and estimation being repeated 100 times.

A relatively large number of Monte Carlo simulations provides more accurate dof estimates with less standard deviations, but the CPU time needed also increases rapidly, especially when thousands of spatial points are involved. When the number of Monte Carlo simulations increases from 1000 to 3000, however, the standard deviation of dof estimates changes very little (from 8 to 5). Therefore, the application of the B method does not require a very large number of Monte Carlo simulations; rather, one may reasonably repeat the estimation process many times and compute the mean and standard deviation of the dof estimate.

d. Comparison using multivariate data

The experiments in previous sections are for a special case since the data's correlation matrix is an identity one. In this section, the general multivariate data are used. They are realizations from a simplified vector autoregressive process,

$$\mathbf{x}_t = \phi \mathbf{x}_{t-1} + [\mathbf{C}]\boldsymbol{\epsilon}_t, \tag{15}$$

in which $\mathbf{x}_t$ and $\mathbf{x}_{t-1}$ are column vectors with dimension N and $\boldsymbol{\epsilon}_t$ is a column vector of independent standard normal distribution with dimension N. Obviously, a data matrix [**X**], which is defined in the first paragraph of section 2, generated this way has a dof less than N, that is, 100 in this section.

As pointed out in Wilks (1997), the (unlagged) correlation matrix of $\mathbf{x}_t$ is $[\mathbf{R}_0] = [\mathbf{C}][\mathbf{C}]^{\mathrm{T}}$. Since ϕ is a constant, the lag-1 autocorrelation matrix is symmetric and proportional to $[\mathbf{R}_0]$. The correlation matrix $[\mathbf{R}_0]$ has as its elements

$$r_{i,j} = r_{|i-j|} = \begin{cases} 1 & |i-j| = 0, \\ s_1/(1-s_2) & |i-j| = 1, \\ s_1 r_{|i-j|-1} + s_2 r_{|i-j|-2} & |i-j| \geq 2. \end{cases} \tag{16}$$

In our experiment, we select $s_1 = 0.8$ and $s_2 = -0.4$. For this correlation matrix $[\mathbf{R}_0]$ and according to the χ^2 method, Eq. (2) provides a dof estimate of 56. This can be treated as the true dof but only for the χ^2 method.

The spatial correlation $r_{|i-j|}$ decreases as $|i-j|$ increases, and $r_{|i-j|}$ oscillates around zero with damped amplitudes. If we take ϕ as zero and [**C**] as an identity matrix, the data matrix generated this way is the same as in previous sections. In general, the matrix [**C**] in Eq. (15) is equal to $[\sqrt{\lambda_n}\mathbf{p}_n]_{n=1}^N$, where $(\sqrt{\lambda_n}, \mathbf{p}_n)$ are eigenpairs of the correlation matrix $[\mathbf{R}_o]$. With this [**C**], the data matrix [**X**] can be generated by Eq. (15) and this data matrix [**X**] is a spatial analog of an autoregression two [AR(2)] process. The dof of [**X**] can be estimated.

Two sets of experiments are conducted, with $\phi = 0$ and $\phi = 0.3$. For each ϕ, 30 data matrices [**X**] are generated. The dimension of each of the 30 matrices [**X**] is $N \times T$ with $N = 100$ but different temporal lengths: $T = 40$, 100, 200, 300, and 1000. The means and standard deviations of the 30 estimated dof's are shown in Table 1. The table demonstrates that when the number of realizations increases, the estimated dof's provided by different methods gradually converge to certain limits. For example, the B method's limit is 73 and the χ^2 method's limit is 56, which are the true dof estimates for the corresponding methods. Since different dof estimation methods use different sample statistics, it is not surprising that the different methods yield different dof estimates, as in the case of estimating the effective sample size for time series data (Thiébaux and Zwiers 1984; Trenberth 1984). Table 1 also indicates that the temporal length T significantly affects the dof estimation by the χ^2 method. For example, when $\phi = 0$, the dof estimate provided by the χ^2 method is 24 when the temporal length is 40. When the temporal length is 1000, the dof estimate is 53, close to the true dof 56. But for the B method, the dof estimate does not sensitively depend on the temporal length T. The maximum dof estimate using the B method for different temporal lengths is 77, and the minimum is 67. In any event, when the temporal length T is large, say 1000, all the estimated dof's approach certain limits.

Not surprisingly, if the lag-1 autocorrelation is included in the vector autoregressive process ($\phi = 0.3$), dof estimates for the B method, χ^2 method, and Z method decrease, especially when the temporal length is 40.

TABLE 1. The mean and standard deviation of estimated spatial degrees of freedom for 30 multivariate data matrices generated according to the same covariance matrix and lag-1 autocorrelation. The number of spatial points of the multivariate data matrix is 100, and its temporal length is taken as 40, 100, 200, 300, 1000. The upper row for each method is for cases with lag-1 autocorrelation ϕ being zero. The lower row for each method is for cases with lag-1 autocorrelation ϕ being 0.3. The multivariate data is a spatial analog of the AR(2) process.

		40		100		200		300		1000	
Length	ϕ	Mean	Std dev	Mean	Std dev	Mean	Std dev	Mean	Std dev	Mean	Std dev
B method	0.0	77.1	7.0	67.3	3.7	69.4	5.7	72.3	5.2	72.9	5.0
	0.3	65.9	6.0	62.9	4.5	67.3	5.7	71.6	5.8	73.5	5.7
χ^2 method	0.0	23.6	0.5	36.3	0.6	44.1	0.4	47.5	0.4	53.2	0.2
	0.3	21.6	0.7	34.0	0.7	42.4	0.5	46.1	0.4	52.7	0.2
S method	0.0	72.0	15.8	67.9	10.6	65.0	7.9	64.0	7.2	63.7	2.6
	0.3	73.1	18.8	68.4	11.4	65.7	7.6	64.5	7.1	64.0	2.9
Z method	0.0	61.4	3.5	58.3	1.3	57.6	0.7	57.3	0.5	57.0	0.2
	0.3	50.0	3.4	52.8	1.4	54.8	0.7	55.4	0.4	56.4	0.2

In this regard, the influence of autocorrelation on the S method is not obvious with large standard deviations of the dof estimates. When the temporal length increases, the dof estimates become quite close to the estimates for the cases of $\phi = 0$. Therefore, the dof estimates obtained by these four methods are mainly related to the field's correlation matrix. Based on the numerical experiments in this section and previous sections, we may conclude that, overall, the B method is an accurate and robust method for dof estimation.

4. Data and computation process

a. Observational data

The four dof estimation methods are applied to the observational data and GCM output. The observational data used are the Combined Land–Ocean Temperature Anomaly Grids (1854–1994) archived at the National Center for Atmospheric Research (NCAR; Jones and Briffa 1992; Jones et al. 1991). The data are monthly temperature anomalies, which are surface air temperature over land and sea surface temperature over ocean. The temperature field is the superposition of the NCAR global temperature grids and Jones's anomaly dataset. The dataset has a spatial resolution of 5° × 5° from 87.5°S to 87.5°N, and from 2.5° to 357.5°E. For the earlier period, the dataset has a sparse spatial coverage, and the period chosen for our analysis is from 1955 to 1994. Those grids having a total number of missing values greater than 48 months (10% of the total 480 months) in 1955–94 are not included in the calculation. The regions for dof investigation are the Northern Hemisphere (NH), the Southern Hemisphere (SH), and the entire globe. The dof is estimated for two timescales: monthly average and annual mean.

Altogether, we use 1002 grid points in the NH (accounting for 77.3% of the NH's total 1296 grid points) and 658 grid points in the SH (accounting for 50.8% of the SH's total 1296 grid points). Figures 4 and 5 show the grid points used in the Northern and the Southern Hemispheres, respectively. The NH has a very good spatial coverage except for the polar region (north of 72.5°N) and the North African region. The SH has a proper spatial coverage of observations over the tropical region and the polar region, but the few dozen grid points over the midlatitude region from 40° to 80°S will affect the dof estimation.

b. GCM data

The analyzed GCM output is the Geophysical Fluid Dynamics Laboratory (GFDL) 100-yr control run (Manabe et al. 1991; Manabe et al. 1992). The model is a general circulation model of the coupled atmosphere–ocean–land surface system with the global geography and seasonal variation of insolation. The field analyzed

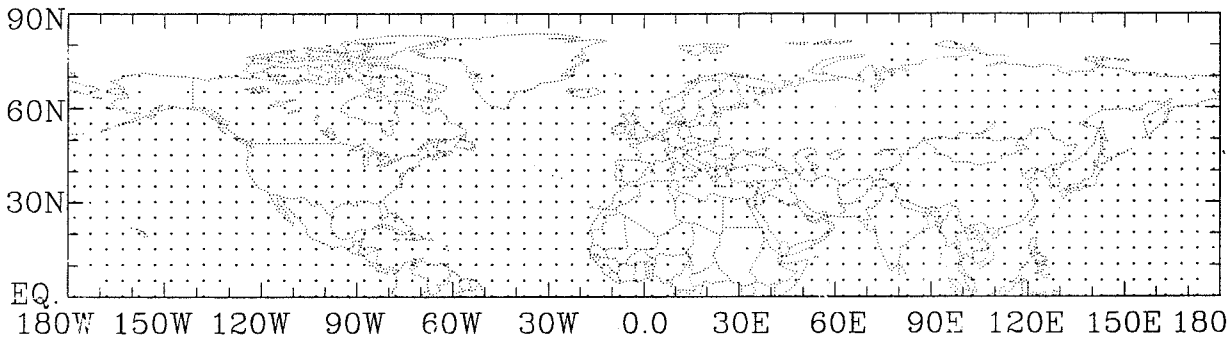

FIG. 4. The distribution of the 1002 grid points used to estimate the spatial dof of the NH monthly surface temperature field (1955–94).

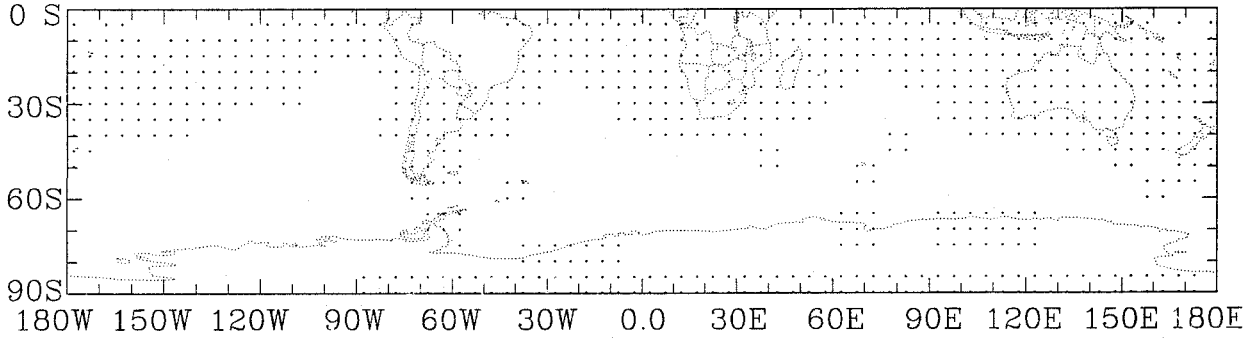

FIG. 5. As in Fig. 4 except for the SH, and the number of grid points used is 658.

is the surface air temperature, which is the temperature at the lowest finite difference level at about 70 m above the surface. The data has a spatial resolution of approximately 4.5° × 7.5° from 87.75°S to 87.75°N and from 3.75° to 356.25°E. The regions for dof estimation are still the NH, the SH, and the entire globe. Both the Northern and the Southern Hemispheres have 960 grid points.

c. Computational process

A preliminary process is carried out before estimating a field's dof. To use the χ^2 method and Z method for observational surface temperature, the data are standardized for each grid point by their mean and standard deviation estimated from the 40-yr period. In the B method, Monte Carlo simulations are conducted 1000 times, and the dof estimation is repeated 100 times to obtain the mean and the standard deviation of the dof estimates. However, for the GCM output, since 100-yr data is used, the CPU time used to conduct the similar computation is very long. Hence, the dof estimation is repeated 50 times to obtain the mean and the standard deviation of the dof estimates. The comparison shows that only slight differences result if the dof estimation is repeated 100 times. The difference of the standard deviations of dof estimates is small. The difference of the means of dof estimates is less than one-half of their standard deviation.

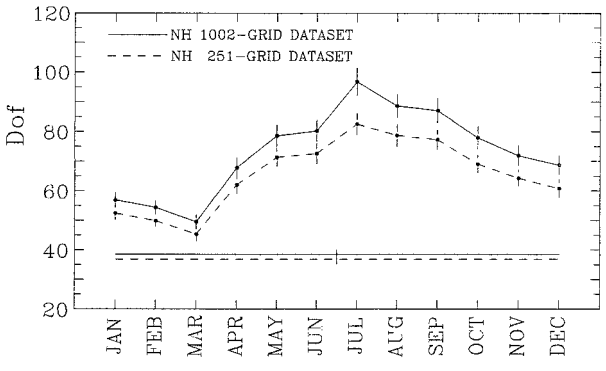

FIG. 6. The mean and standard deviation (vertical lines) of the dof estimated by the B method for the NH monthly surface temperature. The mean and standard deviation of the dof for the annual mean temperature are shown by a straight line and a vertical line on it. The solid lines are for the 1002 gridpoint dataset. The dashed lines are for the reduced 251 gridpoint dataset.

5. Dof estimation of the surface temperature field

a. Northern Hemisphere

The mean and standard deviation of the dof estimated by the B method for the Northern Hemisphere 1002-gridpoint surface temperature dataset are shown in Fig. 6 as solid lines. An annual cycle of the dof is obvious. The minimum dof occurs in March (50), and the maximum in July (97), consistent with the results in Wallace et al. (1993). Their research showed that the leading empirical orthogonal function (EOF) of the winter seasonal mean 500-hPa height presents a well-organized spatial pattern, whereas the leading EOF of summer has the same polarity over almost the entire NH. It should be noted that the standard deviation of the dof estimates is approximately 10% of their mean. This deviation is related to the relationship between m/n and n, which is shown in Fig. 1. When n is large, the value m/n does not change much. Since dof estimation sensitively relies on the estimation of m/n, the number of Monte Carlo simulations should be sufficiently large to obtain a robust estimation. As well, the annual mean temperature has a smaller dof than the monthly average temperature, as shown by the straight solid line in Fig. 6. For the NH, the annual mean temperature has a dof of 38, consistent with the fact that the annual mean temperature has a larger spatial scale. Our results of dof estimation for the monthly mean temperature are comparable to those obtained in earlier research. The estimated dof's for the seasonal average temperature are around 40, with slightly larger values obtained in summertime by using the correlation decay length method (Jones et al. 1997). In Livezey and Chen (1983), the dof's for seasonal average 700-hPa height are 35 for winter and 55 for summer. In their analysis, an estimate of around 30–60 for the dof is also given for the NH, based on the consideration of the number of independent modes (either

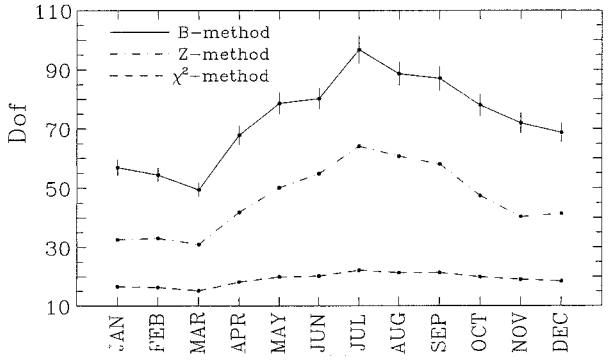

FIG. 7. The dof estimated by the Z method (dash–dotted line), χ^2 method (dashed line), and B method (solid line) for the NH monthly surface temperature.

EOFs or spherical harmonics) needed to account for a high percentage of the total variance of the field. From our analysis, the dof for the NH monthly surface temperature is in the range of 50–110.

The spatial sampling has a minor influence on dof estimation obtained from the B method. Reducing the number of grid points by 50% or even 75% has a minor influence on dof estimation. Of course, the reduced grid points are still evenly distributed over the NH. The dashed lines in Fig. 6 present the dof estimated from the B method when using one-quarter (251) of the total grid points (1002). Figure 6 reveals that the reduced grid points cause a minor change in dof estimation. The estimated dof still has a similar annual cycle. The minimum dof occurs in March (45), and the maximum in July (83). The differences of the means of dof estimates are around 4–14, with larger values in the summer when the dof's are also larger and, hence, have larger standard deviations. The annual mean temperature field has almost the same dof for the original and the reduced grid points.

The dof for the Northern Hemisphere surface temperature is much larger than the results of Van den Dool and Chervin (1986) for the monthly 500-hPa height, obtained from the Z method [the maximum dof in June (37) and the minimum dof in December (14)], and the results for daily datasets [24–44, using the idea of the χ^2 method; Toth (1995); Fraedrich et al. (1995); Lorenz (1969)]. The datasets used by earlier researchers are for height field at higher levels (500, 700, and 200 hPa), whereas our dataset is for surface temperature, which should include more local action centers and have a relatively large dof. The above results are also for different regions, north of 20°N in Lorenz (1969) and 30.5°–74.7°N in Fraedrich et al. (1995). Thus, our work supplements the existing results. The other methods for dof estimation are also applied to the observational data. The dof's estimated by the χ^2 method and Z method are compared in Fig. 7 with the results of the B method. Figure 7 reveals that the dof's estimated by the χ^2 method and Z method have a similar annual cycle as the dof estimated by the B method. However, the dof values are systematically less than those estimated by the B method. For the Z method (dash–dotted line), the dof has a maximum in July (64) and a minimum in March (31). The ratios of the dof's estimated by the Z method to their counterparts estimated by the B method change slightly from 0.56 to 0.68 for different months. In the numerical experiments discussed earlier, the ratio of the dof estimated by the Z method to the true dof is 0.57 for randomly generated data matrices with means and variances that are different from 0 and 1, respectively. If the χ^2 method is used (dashed line), the maximum dof occurs in July (22) and the minimum occurs in March (15). The ratios of the dof's estimated by the χ^2 method to those estimated by the B method for different months are also quite close, from 0.23 to 0.30. These ratios can be compared to the value (0.28) we obtained from using the B method (Fig. 2). This value is the ratio of the estimated dof to the true dof when the number of realizations is 40.

The dof of the NH surface temperature estimated by the S method is quite different from that obtained by using the χ^2 method, Z method, or B method. If the temperature field is used, the estimated dof varies from 17 (March) to 39 (November). If the standardized temperature field is used, the estimated dof varies from 15 (August) to 24 (January). Based on the numerical experiments presented in section 3 and the above analysis, we may conclude that the χ^2 method provides an underestimate of the dof when the number of realizations of the field is not large enough. The Z method and S method will provide an underestimate of the dof when the mean and variance of the field vary with different spatial locations. Therefore, in the following analyses, only the B method is used.

b. Southern Hemisphere

The dof estimated by the B method for the SH surface temperature of the period 1955–94 is much less than that of the NH (solid lines in Fig. 8). The dof of the SH varies from 33 (December) to 41 (June). The annual mean temperature still has the least dof (27). The annual cycle is not clear compared with that of the NH. It appears, that the dof's of its winter months (40; May–July) are even higher than the dof's of its summer months (35; December–February). The data for the period 1958–93 has a larger spatial coverage than that of 1955–94 and has 738 grid points over the SH. The estimated dof obtained by using 1958–93 data is shown in Fig. 8 as dashed lines. Figure 8 reveals that the dof has a minor increase (2–7) because new grid points are included, but the highest dof still occurs in June (48). The lowest dof occurs in December and January (37). At this stage, it is not clear whether the phenomenon is related to the sparse coverage of observations or reflects the real situation of the SH. Figure 5 shows that only a limited number of grid points have data in the mid-

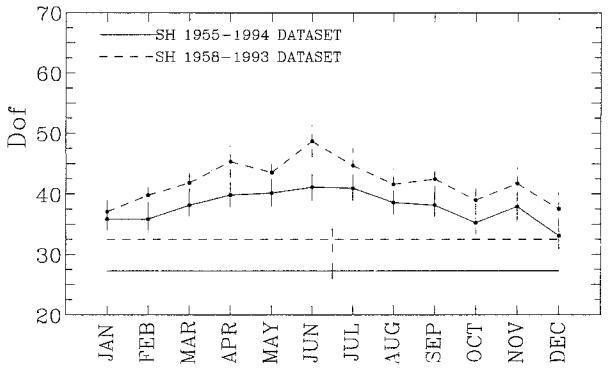

FIG. 8. The mean and standard deviation (vertical lines) of the dof estimated by the B method for the Southern Hemisphere monthly surface temperature. The mean and standard deviation of the dof for the annual mean temperature are shown by a straight line and a vertical line on it. Solid lines are for the 1955–94 dataset, which has 658 grid points. Dashed lines are for the 1958–93 dataset, which has 738 grid points.

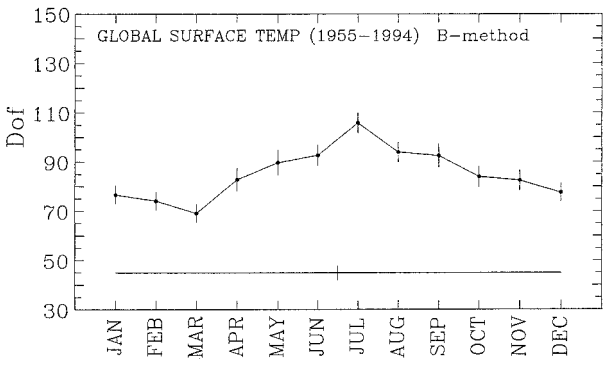

FIG. 9. The mean and standard deviation (vertical lines) of the dof estimated by the B method for the global monthly surface temperature. The mean and standard deviation of the dof for the annual mean temperature are shown by a straight line and a vertical line on it.

latitude of the Southern Hemisphere (42.5°–77.5°S). In this latitude band 82% of the grid points have no data. Notwithstanding the above, this region is ocean, where the temperature field should have a larger spatial scale and each latitudinal band has some grid points. The minimum is 6, which occurs at 57.5°S. Thus, the data coverage is most likely dense enough to provide accurate results. The results in Fraedrich et al. (1995) obtained by using recent daily sea level pressure data from 1980 to 1989 for the Southern Hemisphere (30.5°–74.7°S) support this conclusion. Their results showed that the SH lacks a clear annual cycle and the dof is around 30, with the minimum in February and the maximum in December.

c. Global data

If we merge the data of the NH with those of the SH and estimate the dof for the global surface temperature, the dof of the entire globe should be smaller than the sum of the dof of the NH and the SH since the surface temperature fields of the two hemispheres are not independent, as is shown in Fig. 9. The annual cycle is also clear and shows similar characteristics to those of the annual cycle of the dof of the Northern Hemisphere's surface temperature (Fig. 6). The minimum dof occurs in March (69) and the maximum occurs in July (106). The annual mean temperature again has a smaller dof (45). This low dof for the hemispheric and global surface temperature field is not surprising, given the results of global mean temperature estimation (Jones 1994; Shen et al. 1994).

6. Dof estimation of the GCM output

a. Northern Hemisphere

Figure 10 presents the dof estimates for the GFDL model data over the NH. Compared with the dof of the observational data, the dof of the model output is generally larger. If we consider the fact that the model output used is the temperature 70 m above the surface, the difference is even larger. A similar phenomenon can be noticed in the dof estimation of the seasonal average temperature (Jones et al. 1997) and daily data (Fraedrich et al. 1995). A qualitative explanation is also given in the latter study. Compared with the real atmosphere, the model has a limited number of variables and tends to activate a larger number of its own intrinsic modes to cope with the dynamically required constraints.

In our analysis of climate data, the difference is more obvious in summer than in winter. The greatest difference occurs in June (58), and during the winter from November to February the difference is less than 10, consistent with the results of daily data (Fraedrich et al. 1995). Thus, in terms of the dof, the GFDL model can produce a better simulation for winter than for summer. This result can also be related to the performance of numerical weather prediction that appears, on average, to be better in winter than in summer (Tracton 1993). The annual cycle is reproduced in the GFDL model. The difference is that the minimum dof occurs in January (56) instead of March, and the maximum dof oc-

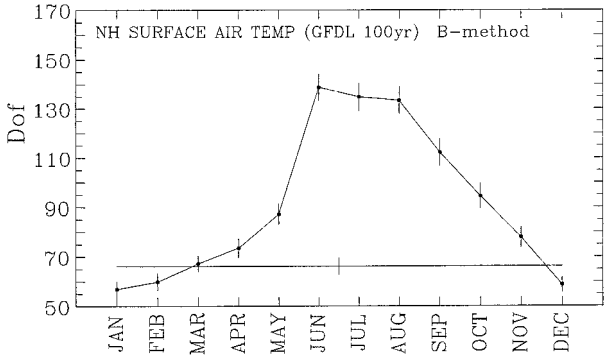

FIG. 10. As in Fig. 9 except for the GFDL 100-yr control run output of the NH monthly surface air temperature.

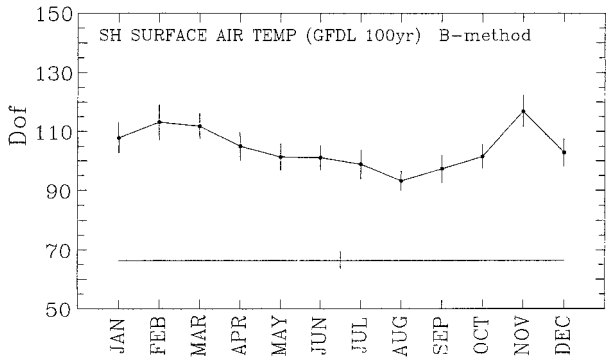

FIG. 11. As in Fig. 10 except for the SH.

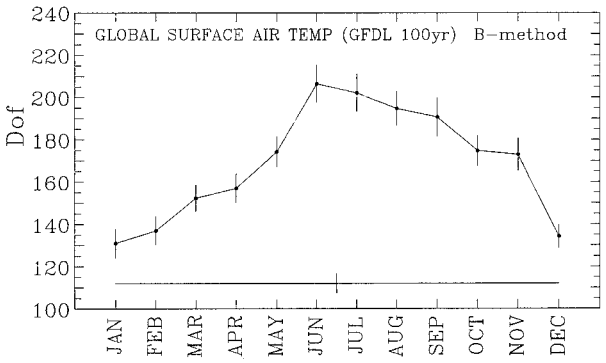

FIG. 12. As in Fig. 10 except for the entire globe.

curs in June (139) instead of July. Another obvious difference is that unlike the observational data, for which the annual mean temperature field has the fewest dof compared with the dof of monthly data, the annual mean temperature of the GFDL model output even has a larger dof than does the monthly data of January, February, and December. The above results may be of interest to the GCM improvement project.

b. Southern Hemisphere

For the SH (Fig. 11), the model output still has a larger dof compared with that of the observations. The dof hovers around 105 for different months. The annual mean temperature has the fewest dof (66). The dof appears to tend to be relatively lower during the winter and relatively higher during the summer. The minimum dof occurs in August (93) and the maximum occurs in November (117). Compared with the dof difference between the model output and the observations in the NH, the difference in the SH is larger. The monthly temperature has a difference of 55–80 with relatively larger values during the summer and smaller values during the winter. The annual cycle presents quite different characteristics compared with the observations. Since the spatial coverage of observations is quite sparse in the SH, we are not sure at this stage how to evaluate the difference between the dof of the observational data and of the model output.

c. Global data

The global temperature field (Fig. 12) still has an obvious annual cycle, with the minimum dof occurring in January (131), and the maximum dof occurring in June (206). The dof for the January temperature field is comparable to that (135) obtained by Madden et al. (1993) by using the correlation decay length method and the NCAR Community Climate Model output of January temperature. The annual mean temperature still has far fewer dof (112) compared with the monthly temperature. The difference between the dof of the model output and that of the observations is around 55–115, with larger values from June to September and smaller values from December to February. It is interesting to note that for the annual mean temperature the model output has the same dof (66) for both the NH and the SH surface air temperature. The difference between the model output's and the observations' dof estimates of the annual mean global temperature field is quite large (67). The discrepancy is rather significant, since the dof for the observational temperature field is 38 for the NH, 27 for the SH, and 45 for the global temperature field.

7. Conclusions and discussion

The comparison of the four selected methods of estimating the spatial degrees of freedom of a climate field shows that the B method can provide a more accurate estimate than the χ^2 method, Z method, and S method. The latter three all result in underestimates when the number of realizations of the field is not sufficiently large or the field has different mean and variance at different spatial locations. Though the standardized data can be used in the application of these methods, these methods still contain large errors when the data's length is very short. The disadvantage of the B method is that when the number of Monte Carlo simulations is not sufficiently large, the estimate is not robust, but in principle, at this stage of computer development and for the climate field of large spatial scales, this disadvantage is not a major problem. By repeating the B method for a sufficient number of times, the standard deviation of the dof estimates can be estimated. In our analysis, the number of Monte Carlo simulations is 1000. The standard deviation of the dof estimates is around 10% of their mean, which is a reasonable estimate.

The B method's dof estimation of the observational monthly surface temperature shows that the dof of the NH has an obvious annual cycle, with values around 60 in the winter and 90 in the summer. For the SH the dof changes from 35 to 50, and the annual cycle is not clear. It appears that the dof's of the SH's winter months are greater than the dof's of its summer months. For the global temperature field, the dof is less than the sum of the dof of the two hemispheres, implying a correlation

between them. The dof of the global temperature field has an obvious annual cycle similar to that in the NH, with dof around 75 from December to March and around 95 from June to September.

The dof for the GFDL model output of the surface air temperature is generally larger than that of the observational data. For the NH, the difference is around 10–60, with larger values in its summer months. For the SH, the difference is around 55–80, with larger values also in its summer months. One obvious difference between the dof's of the model output and the observations is that the annual mean temperature for the NH has a larger dof than that of the monthly mean temperature in winter months. Another difference is that for the SH the dof of the model output has a weak annual cycle with a dof around 100 for its winter months and around 110 for its summer months. It is not clear yet whether this difference is caused by the sparse spatial coverage of the observational data over the Southern Hemisphere midlatitude region.

Acknowledgments. The research was supported by Natural Sciences and Engineering Research Council of Canada and Atmospheric and Environmental Service of Canada. The authors thank two anonymous reviewers whose suggestions helped to improve the manuscript significantly.

REFERENCES

Bell, T. L., 1986: Theory of optimal weighting of data to detect climatic change. *J. Atmos. Sci.,* **43,** 1694–1710.

Fraedrich, K., C. Ziehmann, and F. Sielmann, 1995: Estimates of spatial degrees of freedom. *J. Climate,* **8,** 361–369.

Hansen, J., and S. Lebedeff, 1987: Global trends of measured surface air temperature. *J. Geophys. Res.,* **92,** 13 345–13 372.

Horel, J. D., 1985: Persistence of the 500 mb height field during Northern Hemisphere winter. *Mon. Wea. Rev.,* **113,** 2030–2042.

Jones, P. D., 1994: Hemispheric surface air temperature variation: A reanalysis and an update to 1993. *J. Climate,* **7,** 1794–1802.

——, and K. R. Briffa, 1992: Global surface air temperature variations over the twentieth century, Part I: Spatial, temporal and seasonal details. *Holocene,* **2,** 165–179.

——, S. C. B. Raper, R. S. Bradley, H. F. Diaz, P. M. Kelly, and T. M. L. Wigley, 1986a: Northern Hemisphere surface air temperature variations: 1851–1984. *J. Climate Appl. Meteor.,* **25,** 161–179.

——, ——, ——, ——, ——, and ——, 1986b: Southern Hemisphere surface air temperature variations: 1851–1984. *J. Climate Appl. Meteor.,* **25,** 1213–1230.

——, T. M. L. Wigley, and G. Farmer, 1991: Marine and land temperature data sets: A comparison and a look at recent trends. *Greenhouse-Gas-Induced Climatic Change: A Critical Appraisal of Simulations and Observations,* M. E. Schlesinger, Ed., Elsevier, 153–172.

——, T. J. Osborn, and K. R. Briffa, 1997: Estimating sampling errors in large-scale temperature averages. *J. Climate,* **10,** 2548–2568.

Kim, K.-Y., and G. R. North, 1991: Surface temperature fluctuations in a stochastic climate model. *J. Geophys. Res.,* **96,** 18 573–18 580.

Livezey, R. E., and W. Y. Chen, 1983: Statistical field significance and its determination by Monte Carlo techniques. *Mon. Wea. Rev.,* **111,** 49–59.

Lorenz, E. N., 1969: Atmospheric predictability as revealed by naturally occurring analogues. *J. Atmos. Sci.,* **26,** 636–646.

Madden, R. A., D. J. Shea, G. W. Branstator, J. J. Tribbia, and R. O. Weber, 1993: The effects of imperfect spatial and temporal sampling on estimates of the global mean temperature: Experiments with model data. *J. Climate,* **6,** 1057–1066.

Manabe, S., R. J. Stouffer, M. J. Spelman, and K. Bryan, 1991: Transient response of a coupled ocean–atmosphere model to gradual changes of atmospheric CO_2. Part I: Annual mean response. *J. Climate,* **4,** 785–818.

——, M. J. Spelman, and R. J. Stouffer, 1992: Transient response of a coupled ocean–atmosphere model to gradual changes of atmospheric CO_2. Part II: Seasonal response. *J. Climate,* **5,** 105–126.

North, G. R., T. L. Bell, R. F. Cahalan, and F. J. Moeng, 1982: Sampling errors in the estimation of empirical orthogonal functions. *Mon. Wea. Rev.,* **110,** 699–706.

Sachs, L., 1984: *Applied Statistics: A Handbook of Techniques.* 2d ed. Springer-Verlag, 707 pp.

Shen, S. S. P., G. R. North, and K.-Y. Kim, 1994: Spectral approach to optimal estimation of the global average temperature. *J. Climate,* **7,** 1999–2007.

Smith, T. M., R. W. Reynolds, and C. F. Ropelewski, 1994: Optimal averaging of seasonal sea surface temperatures and associated confidence intervals (1860–1989). *J. Climate,* **7,** 949–964.

Thiébaux, H. J., and F. W. Zwiers, 1984: The interpretation and estimation of effective sample size. *J. Climate Appl. Meteor.,* **23,** 800–811.

Toth, Z., 1995: Degrees of freedom in Northern Hemisphere circulation data. *Tellus,* **47A,** 457–472.

Tracton, M. S., 1993: On the skill and utility of NMC's medium-range central guidance. *Wea. Forecasting,* **8,** 147–153.

Trenberth, K. E., 1984: Some effects of finite sample size and persistence on meteorological statistics. Part I: Autocorrelations. *Mon. Wea. Rev.,* **112,** 2359–2368.

Van den Dool, H. M., and R. M. Chervin, 1986: A comparison of month-to-month persistence of anomalies in a general circulation model and in the earth's atmosphere. *J. Atmos. Sci.,* **43,** 1454–1466.

Vinnikov, K. Ya., P. Ya. Groisman, and K. M. Lugina, 1990: Empirical data on contemporary global climate changes (temperature and precipitation). *J. Climate,* **3,** 662–677.

Wallace, J. M., Y. Zhang, and K.-H. Lau, 1993: Structure and seasonality of interannual and interdecadal variability of the geopotential height and temperature field in the Northern Hemisphere troposphere. *J. Climate,* **6,** 2063–2082.

Wilks, D. S., 1997: Resampling hypothesis tests for autocorrelated fields. *J. Climate,* **10,** 65–82.